Robust controller for interleaved DC-DC converters and buck inverter in Grid-Connected Photovoltaic Systems

HASSAN ABOUOBAIDA, MOHAMED CHERKAOUI
Department of Electrical Engineering,
Mohamed V University, Ecole Mohamedia d'ingénieur
RABAT, MOROCCO
Email: Hassan_abouobaida@yahoo.fr , Cherkaoui@emi.ac.ma

Abstract—The present work describes the analysis, modeling and control of an interleaved Boost converters and Buck power inverter used as a DC-DC and DC-AC power conditioning stage for grid-connected photovoltaic (PV) systems. To maximize the steady-state input-output energy transfer ratio a backstepping controller is designed to assure output unity power factor and a Maximum Power Point Tracking (MPPT) algorithm to optimize the PV energy extraction. The achievement of the DC-AC conversion at unity power factor and the efficient PV's energy extraction are validated with simulation results.

Keywords: MPPT, unity power factor, backstepping controller, Lyapunov

1. Introduction

Many renewable energy technologies today are well developed, reliable, and cost competitive with the conventional fuel generators. The cost of renewable energy technologies is on a falling trend as demand and production increases. There are many renewable energy sources such as solar, biomass, wind, and tidal power. The solar energy has several advantages for instance clean, unlimited, and its potential to provide sustainable electricity in area not served by the conventional power grid.

However, the solar energy produces the dc power, and hence power electronics and control equipment are required to convert dc to ac power. There are two types of the solar energy system, stand-alone power system and grid-connected power system. Both systems have several similarities, but are different in terms of control functions. The stand-alone system is used in off-grid application with battery storage. Its control algorithm must have an ability of bidirectional operation, which is battery charging and inverting.

There are three main types of switched power converters respectively called Boost, Buck and Buck-Boost. These have recently aroused an increasing deal of interest both in power electronics and in automatic control. This is due to their wide applicability domain that ranges from domestic equipments to sophisticated communication systems. They are also used in computers, industrial electronics, battery operating portable equipments and uninterruptible power sources. From an automatic control viewpoint, a switched power converter constitutes an interesting case study as it is a variable-structure nonlinear system. Its rapid structure variation is accounted for using averaged models.

Based on these, Several controller strategies have been used in the literature, citing the PI in [2] that is generally suitable for linear systems, the sliding mode in [3]-[4] for which the chattering problem, and fuzzy logic proposed adjustment in adapted to systems without a mathematical model [4].

In order to extract the maximum amount of energy the PV system must be capable of tracking the solar array's maximum power point (MPP) that varies with the solar radiation value and temperature. Several MPPT algorithms have been proposed [5], namely, Hill Climbing algorithm [6], Perturb and Observe (P&O) [7], incremental conductance [8], fuzzy based algorithms [9], RCC (Ripple Correlation Control) [10]-[11], etc. They differ from its complexity and tracking accuracy but they all required sensing the PV current and/or the PV voltage.

Recently, dc–dc converters with steep voltage ratio are usually required in many industrial applications. One approach to constructing a large power converter system is the use of a cellular architecture, in which many quasi-autonomous converters, called cells, are paralleled to create a single large converter system. The use of quasi-autonomous cells means that system performance is not compromised by the failure of a cell. One of the primary benefits of a cellular conversion approach is the large degree of input and output ripple cancellation which can be achieved among cells, leading to reduced ripple in the aggregate input and output waveforms. The active method of interleaving permits to obtain more advantages. In the interleaving method, the cells are operated at the same switching frequency with their switching waveforms displaced in phase over a switching period. The benefits of this technique are due to harmonic cancellation among the cells, and include low ripple amplitude and high ripple frequency in the aggregate input and output waveforms. For a broad class of topologies, interleaved operation of N cells yields an N-fold increase in fundamental current ripple frequency, and a reduction in peak ripple magnitude by a factor of N or more compared to synchronous operation. To be effective in cellular converter architecture, however, an interleaving scheme must be able to accommodate a varying number of cells and maintain operation after some cells have failed [12].

The problem of controlling switched power converters is approached using the backstepping technique [13]. While feedback linearization methods require precise models and often cancel some useful nonlinearities, backstepping designs offer a choice of design tools for accommodation of uncertain nonlinearities and can avoid wasteful cancellations. The backstepping approach is applied to a specific class of switched power converters, namely dc-to-dc boost converters. In the case where the converter model is fully known the backstepping nonlinear controller is shown to achieve the control objectives i.e. input voltage tracking and robustness with respect to climate change uncertainty.

In this paper, a backstepping control strategy is developed to track the maximum power of a solar generating system and to assure that the output current presents both low harmonic distortion and robustness in front of system's perturbations.

Nomenclature

u_{c2}	DC voltage
u_{c2}*	Desired DC voltage
u_{pv1}	PV voltage
u_{pv1}*	desired PV voltage
i_{pv1}	PV current
i_{L1}	Inductor current
i_{L1}*	Desired Inductor current
c_1	Capacitance
c_2	Capacitance
u_r	Grid voltage
i_r	output current
i_r*	Desired output current
u_1, u_2	switched control signal
α	duty cycle of boost converter
β	duty cycle of buck inverter
k_1, k_2, k_{11}, k_{22}	design parameter
e_1	error $u_{pv1} - u_{pv1}$*
e_2	error $i_{L1} - i_{L1}$*
e_{11}	error u_{c2}-u_{c2}*
e_{22}	error i_r-i_r*
v	Lyapunov function
α_1	stabilization function
R_p	parallel resistance of PV cell
R_s	series resistance of PV cell

The desired array voltage is designed online using a P&O MPPT tracking algorithm.

The proposed strategy ensures that the MPP is determined and the system errors are globally asymptotically stable. The stability of the control algorithm is verified by Lyapunov analysis [13].

The rest of the paper is organized as follows. The dynamic model of the global system (PV array, boost converter, buck inverter) is described in Section 2. A control design, backstepping controller of boost converter, buck converter are designed along with the corresponding closed-loop error system and the stability analysis is discussed in Section 3, 4 and 5 respectively. In Section 6, a simulation results and comments are presented.

2. MPPT System Modeling

The multi-string inverter depicted in Figure1 is the further development of the string inverter, where several strings are interfaced with their own dc–dc converter to a common dc–ac inverter. This is beneficial, compared with the centralized system, since every string can be controlled individually. Thus, the operator may start his/her own PV power plant with a few modules. Further enlargements are easily achieved since a new string with dc–dc converter can be plugged into the existing platform. A flexible design with high efficiency is hereby achieved [12].

The solar generation model consists of a PV array module, interleaved dc-dc boost converter and a dc-ac buck inverter as shown in Figure 1.

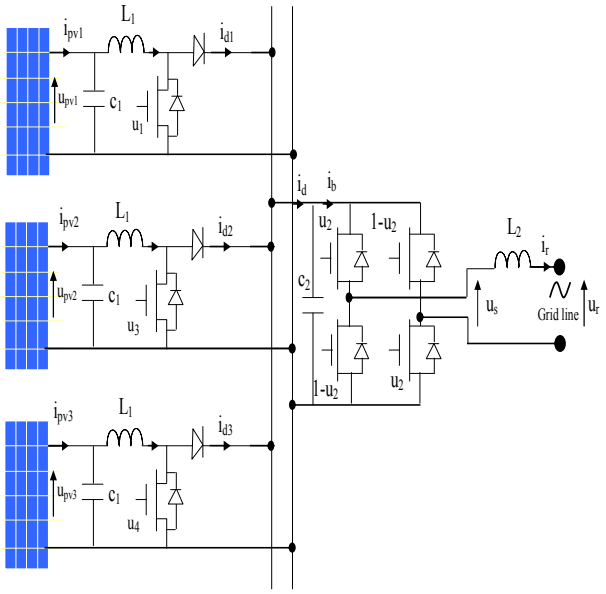

Fig.1. Interleaved boost converter connected to full bridge buck inverter

2.3 PV model

PV cell is a p-n junction semiconductor, which converts light into electricity. When the incoming solar energy exceeds the band-gap energy of the module, photons are absorbed by materials to generate electricity. The equivalent-circuit model of PV is shown in Figure 2. It consists of a light-generated source, diode, series and parallel resistances [14]-[15].

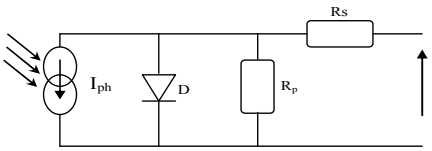

Fig.2. Equivalent model of solar cell

2.3 Boost model

The dynamic model of the solar generation system presented in figure 3 can be expressed by an instantaneous switched model as follows [3]:

$$c_1 . \dot{u}_{pv1} = i_{pv1} - i_{L1}$$
$$L . i_{L1} = u_{pv1} - (1 - u_1) . u_{c2} \quad (1)$$

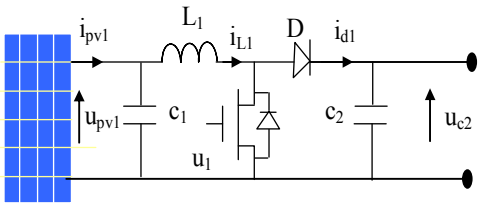

Fig.3. PV array connected to boost converter

where L_1 and i_{L1} represents the first dc-dc converter storage inductance and the current across it, u_{c2} is the DC bus voltage and u_1 is the switched control signal that can only take the discrete values 0 (switch open) and 1 (switch closed).

Using the state averaging method, the switched model can be redefined by the average PWM model as follows:

$$c_1 . \dot{u}_{pv1} = i_{pv1} - i_{L1} \quad (2)$$
$$L . i_{L1} = u_{pv1} - \alpha . u_{c2} \quad (3)$$

Where α is averaging value of $(1\text{-}u_1)$, u_{pv1} and i_{pv1} are the average states of the output voltage and current of the solar cell, i_{L1} is the average state of the inductor current.

2.3 Inverter model

The active power transfer from the PV panels is accomplished by power factor correction (line current in phase with grid voltage). The inverter operates as a current-control inverter (CCI). Noticing that u_2 stand for the control signal of buck inverter, the system can be represented by equations (4) [16].

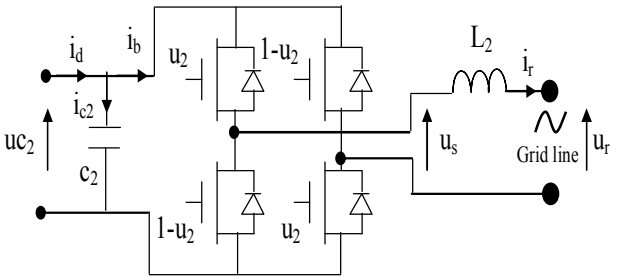

Fig.4. Buck inverter connected to grid line

$$
\begin{aligned}
& c_2 .\dot{u}_{c2} = i_d - i_b \\
& L_2 .\dot{i}_r = u_s - u_r \\
& u_s = (2.u_2 - 1) . u_{c2} \\
& i_b = (2.u_2 - 1) . i_r \\
& i_d = i_{d1} + i_{d2} + i_{d3}
\end{aligned} \qquad (4)
$$

Where uc_2, u_s, u_r designs a DC voltage, output inverter voltage and AC grid voltage, respectively. And i_d, i_b, i_r are converter output current, inverter input current and grid current respectively and u_2 is the switched control signal that can only take the discrete values 0 (switch open) and 1 (switch closed).
Using the state averaging method (on cutting period), the switched model can be redefined by the average PWM model as follows:

$$c_2 . \frac{\dot{X}}{2} = i_d .u_{c2} - u_s .i_r \qquad (5)$$

$$L_2 .\dot{i}_r = \beta . u_{c2} - u_r \qquad (6)$$

Where β is averaging value of $(2.u_2 - 1)$ and X is the square of the DC voltage.

3. Control design

Two main objectives have to be fulfilled in order to transfer efficiently the photovoltaic generated energy into the utility grid are tracking the PV's maximum power point (MPP) and obtain unity power factor and low harmonic distortion at the output. Figure 5 shows the control scheme used to accomplish the previous objectives [16].
The interleaved boost converters are governed by control signal α_i (i □ [1..3]) generated by backstepping controller. This controller is developed to maximize the power of the solar generating system.
The controller tracks a desired array voltage designed online by using MPPT algorithm, by varying the duty cycle of the switching converter.
The unity power factor controller input signal u_2 that controls the buck inverter. This controller consists of an inner current loop and an outer voltage loop. The inner current loop is responsible of obtaining a unitary power factor. The outer voltage loop assures a steady-state maximum input-output energy transfer ratio and a desired steady-state averaged DC-link voltage guarantying proper Buck inverter dynamics [16].

4. Backstepping controller for boost converter

The boost converter is governed by control signal α generated by a backstepping controller that allow to extract maximum of photovoltaic generator control by regulating the voltage of the photovoltaic generator to

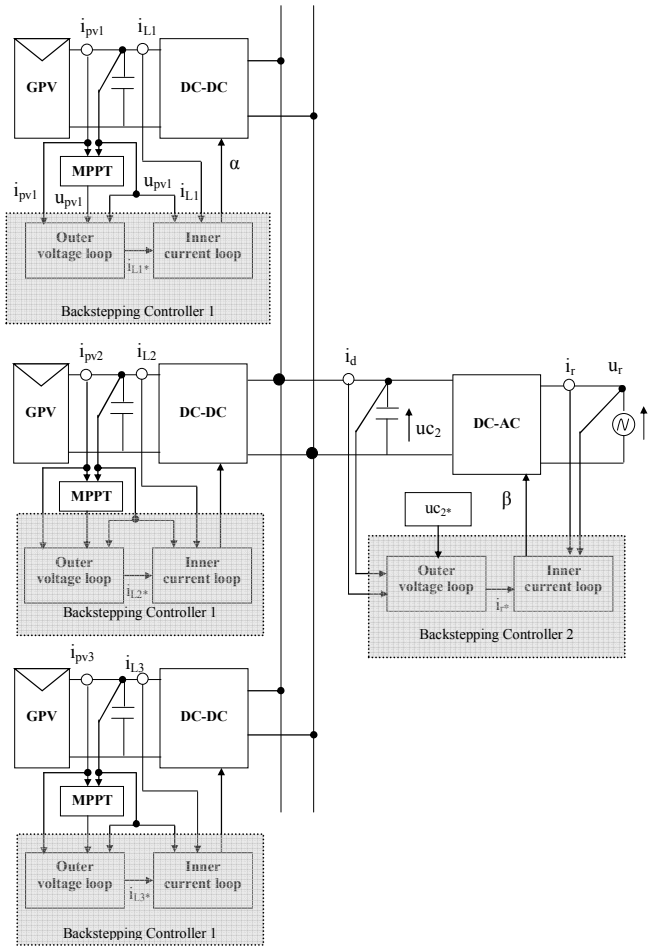

Fig.5. Control scheme

its reference provided by conventional P&O MPPT algorithm as illustrated in figure 6.

Step 1. Let us introduce the input error :

$$e_1 = u_{pv1} - u_{pv1}^*$$

Deriving e_1 with respect to time and accounting for (2) and (3), implies:

$$\dot{e}_1 = \dot{u}_{pv1} - \dot{u}_{pv1}^* = \frac{i_{pv1}}{c_1} - \frac{i_{L_1}}{c_1} - \dot{u}_{pv1}^* \qquad (7)$$

In equation (7), i_{L1} behaves as a virtual control input. Such an equation shows that one gets $\dot{e}_1 = -k_1.e_1$ ($k_1>0$ being a design parameter) provided that:

$$i_{L_1} = k_1.c_1.e_1 + i_{pv1} - c_1.\dot{u}_{pv1}^* \qquad (8)$$

As i_{L1} is just a variable and not (an effective) control input, (7) cannot be enforced for all $t\geq 0$. Nevertheless, equation (7) shows that the desired value for the variable i_{L1} is :

$$\alpha_1 = i_{L_1}^* = k_1.c_1.e_1 + i_{pv1} - c_1.\dot{u}_{pv1}^* \qquad (9)$$

Indeed, if the error:

$$e_2 = i_{L_1} - i_{L_1}^* \qquad (10)$$

vanishes (asymptotically) then control objective is achieved i.e. $e_1 = u_{pv1} - u_{pv1}^*$ vanishes in turn. The desired value α_1 is called a stabilization function.

Now, replacing i_{L1} by $(e_2+i_{L1}^*)$ in (7) yields :

$$\dot{e}_1 = \frac{i_{pv1}}{c_1} - \frac{(i_{L_1}^* + e_2)}{c_1} - \dot{u}_{pv1}^*$$

which, together with (9), gives:

$$\dot{e}_1 = -k_1.e_1 - \frac{e_2}{c_1} \qquad (11)$$

Step 2. Let us investigate the behaviour of error variable e_2.

In view of (3) and (10), time-derivation of e_2 turns out to be:

$$\dot{e}_2 = \dot{i}_{L_1} - \dot{i}_{L_1}^* = \frac{u_{pv1}}{L_1} - \frac{\alpha.u_{c2}}{L_1} - \dot{i}_{L_1}^* \qquad (12)$$

From (9) one gets:

$$\dot{\alpha}_1 = \dot{i}_{L_1}^* = k_1.c_1.\dot{e}_1 + \dot{i}_{pv1} - c_1.\ddot{u}_{pv1}^*$$

which together with (12) implies:

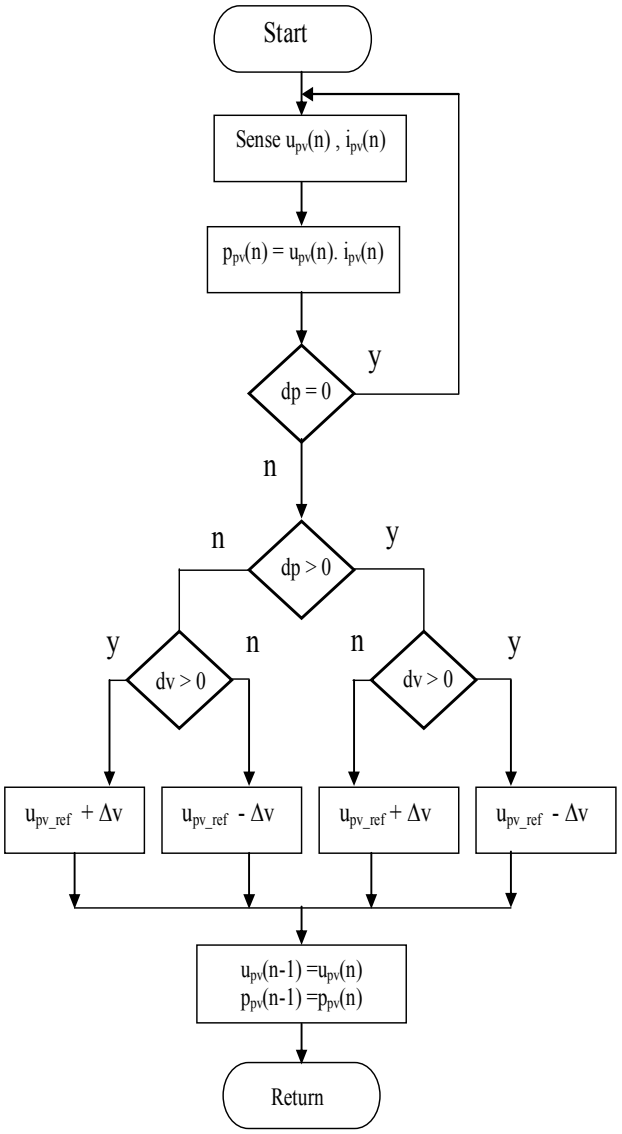

Fig.6. Flowchart of MPPT algorithm

$$\dot{e}_2 = \frac{u_{pv1}}{L_1} - \frac{\alpha.u_{c2}}{L_1} - k_1.c_1.\dot{e}_1 - \dot{i}_{pv1} + c_1.\ddot{u}_{pv1}^* \qquad (13)$$

In the new coordinates (e_1,e_2), the controlled system (1) is expressed by the couple of equations (11) and (13). We now need to select a Lyapunov function for such a system. As the objective is to drive its states (e_1,e_2) to zero, it is natural to choose the following function:

$$v = \frac{1}{2}.{e_1}^2 + \frac{1}{2}.{e_2}^2$$

The time-derivative of the latter, along the (e1,e2) trajectory, is:

$$\dot{v} = e_1.\dot{e}_1 + e_2.\dot{e}_2$$

$$\dot{v} = -k_1.e_1^2 - k_2.e_2^2$$

$$+e_2.\left[\frac{u_{pv1}}{L_1} - \frac{\alpha u_{c2}}{L_1} - k_1.c_1.\dot{e}_1 - \frac{e_1}{c_1} - \dot{i}_{pv1} + c_1.\ddot{u}_{pv1}^* + k_2.e_2\right] \quad (14)$$

where $k_2>0$ is a design parameter and $\dot{e}_2$ is to be replaced by the right side of (13). Equation (14) shows that the equilibrium (e1,e2) = (0,0) is globally asymptotically stable if the term between brackets in (14) is set to zero. So doing, one gets the following control law:

$$\alpha = \frac{L_1}{u_{c2}}\left[\frac{u_{pv1}}{L_1} - k_1.c_1.\dot{e}_1 - \frac{e_1}{c_1} - \dot{i}_{pv1} + c_1.\ddot{u}_{pv1}^* + k_2.e_2\right] \quad (15)$$

Proposition : Consider the control system consisting of the average PWM Boost model (2)-(3) in closed-loop with the controller (15), where the desired input voltage reference u_{pv1}^* is sufficiently smooth and satisfies $u_{pv1}^*>0$. Then, the equilibrium $i_{L1} \rightarrow i_{L1}^*$, $u_{pv1} \rightarrow u_{pv1}^*$ and $\alpha \rightarrow \alpha_0$ is locally asymptotically stable where :

$$\alpha_0 = \frac{L_1}{u_{c2}}\left[\frac{u_{pv1}}{L_1} - \dot{i}_{pv1} + c_1.\ddot{u}_{pv1}^*\right] \quad (16)$$

5. Backstepping controller for buck inverter

The unity power factor controller input signal u_2 that controls the buck inverter. This controller consists of an inner current loop and an outer voltage loop. The inner current loop is responsible of obtaining a unitary power factor. The outer voltage loop assures a steady-state maximum input-output energy transfer ratio and a desired steady-state averaged DC-link voltage guarantying proper Buck inverter dynamics [16].

Step 1. Let us introduce the input error :

$$e_{11} = X - X^* \quad (17)$$

Where X* is a reference signal of square of DC voltage witch to be equal the square value of input inverter voltage (u_{c2} must be higher than the grid voltage).

Deriving e_{11} with respect to time and accounting for (5) implies:

$$\dot{e}_{11} = \dot{X} - \dot{X}^* = 2.\frac{i_d.u_{c2}}{c_2} - 2.\frac{u_s.i_r}{c_2} \quad (18)$$

In equation (18), i_r behaves as a virtual control input. Such an equation shows that one gets $\dot{e}_{11}=-k_{11}.e_{11}$ ($k_{11}>0$ being a design parameter) provided that:

$$i_r = \frac{k_{11}.c_2.e_{11} + 2.u_{c2}.i_d}{2.u_s} \quad (19)$$

As i_r is just a variable and not (an effective) control input, (19) cannot be enforced for all $t\geq 0$. Nevertheless, equation (19) shows that the desired value for the variable i_r is:

$$\alpha_{11} = i_r^* = \frac{k_{11}.c_2.e_{11} + 2.u_{c2}.i_d}{2.u_r} \quad (20)$$

The equality of average (on cutting period) inverter output power ($p_i=\langle u_s.i_r\rangle$) and grid input power ($p_g=\langle u_r.i_r\rangle$) implies $\langle u_r\rangle=\langle u_s\rangle$.

Indeed, if the error:

$$e_{22} = i_r - i_r^* \quad (21)$$

vanishes (asymptotically) then control objective is achieved i.e. $e_{11}=u_{c2}-u_{c2}^*$ vanishes in turn. The desired value α_{11} is called a stabilization function.
Now, replacing i_r by $(i_r^*+e_{22})$ in (18) yields :

$$\dot{e}_{11} = 2.\frac{i_d.u_{c2}}{c_2} - 2.\frac{u_r.(i_r^* + e_{22})}{c_2} \quad (22)$$

which, together with (20), gives:

$$\dot{e}_{11} = -k_{11}.e_{11} - \frac{u_r}{c_2}.e_{22} \quad (23)$$

Step 2. Let us investigate the behavior of error variable e_{22}.
In view of (4), time-derivation of e_{22} turns out to be:

$$\dot{e}_{22} = \dot{i}_r - \dot{i}_r^* = \frac{\beta.u_{c2} - u_r}{L_2} - \dot{i}_r^* \quad (24)$$

From (20) one gets:

$$\dot{\alpha}_1 = \dot{i}_r^* = \frac{u_r.(k_{11}.c_2.\dot{e}_{11} + 2.\dot{i}_d.u_{c2} + 2.i_d.\dot{u}_{c2})}{2.u_r^2} - \frac{\dot{u}_r.(k_{11}.c_2.e_{11} + 2.i_d.u_{c2})}{2.u_r^2} \quad (25)$$

which together with (24) implies:

$$\dot{e}_{22} = \frac{\beta.u_{c2} - u_r}{L_2} - \frac{u_r.(k_{11}.c_2.\dot{e}_{11} + 2.\dot{i}_d.u_{c2} + 2.i_d.\dot{u}_{c2})}{2.u_r^2} + \frac{\dot{u}_r.(k_{11}.c_2.e_{11} + 2.i_d.u_{c2})}{2.u_r^2} \quad (26)$$

In the new coordinates (e_{11},e_{22}), the controlled system is expressed by the couple of equations (23) and (26). We now need to select a Lyapunov function for such a system. As the objective is to drive its states (e_{11},e_{22}) to zero, it is natural to choose the following function:

$$v = \frac{1}{2}.e_{11}^2 + \frac{1}{2}.e_{22}^2 \quad (27)$$

The time-derivative of the latter, along the (e_{11},e_{22}) trajectory (using (23) and (26)) is:

$$\dot{v} = e_{11}.\dot{e}_{11} + e_{22}.\dot{e}_{22}$$

$$\dot{v} = -k_{11}.e_{11}^2 - k_{22}.e_{22}^2 + e_{22}.\left[\frac{\beta.u_{c2} - u_r}{L_2} - \frac{u_r.(k_{11}.c_2.\dot{e}_{11} + 2.\dot{i}_d.u_{c2} + 2.i_d.\dot{u}_{c2})}{2.u_r^2} + \frac{\dot{u}_r.(k_{11}.c_2.e_{11} + 2.i_d.u_{c2})}{2.u_r^2} - \frac{u_r.e_{11}}{c_2}\right] \quad (28)$$

where $k_{22}>0$ is a design parameter and $\dot{i}_r$ is to be replaced by the right side of (25). Equation (28) shows that the equilibrium (e_{11},e_{22}) = (0,0) is globally asymptotically stable if the term between brackets in (28) is set to zero. So doing, one gets the following control law:

$$\beta = \frac{L_2}{u_{c2}}.\left[\frac{u_r}{L_2} + \frac{u_r.(k_{11}.c_2.\dot{e}_{11} + 2.\dot{i}_d.u_{c2} + 2.i_d.\dot{u}_{c2})}{2.u_r^2} - \frac{\dot{u}_r.(k_{11}.c_2.e_{11} + 2.i_d.u_{c2})}{2.u_r^2} + \frac{u_r.e_{11}}{c_2}\right] \quad (29)$$

Proposition : Consider the control system consisting of the average PWM Buck model in closed-loop with the controller (29), where the desired DC voltage reference u_{c2}^* is sufficiently smooth. Then, the equilibrium $i_r \rightarrow i_r^*$, $u_{c2} \rightarrow u_{c2}^*$ and $\beta \rightarrow \beta_0$ is globally asymptotically stable where:

$$\beta_0 = \frac{L_2}{u_{c2}}.\left[\frac{u_r}{L_2} + \frac{u_r.(2.\dot{i}_d.u_{c2} + 2.i_d.\dot{u}_{c2}) - 2.\dot{u}_r.i_d.u_{c2}}{2.u_r^2}\right] \quad (30)$$

6. Simulation result

The PV model, interleaved boost converter, buck inverter model, backstepping controller and P&O MPPT algorithm are implemented in Matlab/Simulink as illustrated in Figure 5. In the study, RSM-60 PV module has been selected as PV power source, and the parameter of the components are chosen to deliver maximum 3kW of power generated by connecting 16 module of RSM-60 in parallel (1kw for each converter). Each boost converter operates at a maximum power point separately to other converters. The specification of the system and PV module are respectively summarized in the following tables.

TABLE I
MAIN CHARACTERISTICS OF THE PV GENERATION SYSTEM

Maximum power	Output voltage at P_{max}	Open-circuit voltage	Short current circuit
60w	16v	21.5v	3.8A

TABLE II
CONTROL PARAMETERS USED IN THE SIMULATION

parameters	Value	unit
k_1	100	
k_2	11000	
k_{11}	1000	
k_{22}	10000	
c_1	220	µF
c_2	4700	µF
L_1	0.001	H
L_2	0.002	H
u_r	220/50	V / Hz

A Matlab simulation of the complete system with the backstepping controller and the MPPT algorithm has been carried out using the following parameters:
• Buck switching frequency = 25kHz
• Boost switching frequency = 100kHz

The proposed controller is evaluated from tow aspects: robustness to irradiance and temperature. In each figures, two different values of irradiance and temperature are introduced in order to show the robustness. Figure 7 shows the simulation results of the designed interleaved boost converter and buck inverter when the solar radiation changes from 500W/m^2 to 1000W/m^2 and then the temperature change from 25°c to 30°c at t=2s and t=2.5s respectively. Figure 7.c shows that the DC-link capacitor voltage reaches the commanded value of 450V witch is greater than AC grid voltage. Figure 7.d shows the influence of temperature on the power transmitted to the grid. This power degrades slightly with increasing temperature.
Notice that according to figure 7.d the maximum power point is always reached after a smooth transient response and the power of photovoltaic generator reaches the commanded value according to radiation change and temperature,
From figure 8.a and figure 8.b, it can be seen that the output current is in phase with the utility grid voltage.

Conclusions

A backstepping control strategy has been developed for a solar generating system to inject the power extracted from a photovoltaic array and obtain unitary power factor in varying weather conditions. A desired array voltage is designed online using an MPPT searching algorithm to seek the unknown optimal array voltage. To track the designed trajectory, a tow backstepping controller are developed to modulate the duty cycle of the interleaved boost converters and buck inverter. The proposed controller is proven to yield global asymptotic stability with respect to the tracking errors via Lyapunov analysis. Simulation results are provided to verify the effectiveness of this approach.

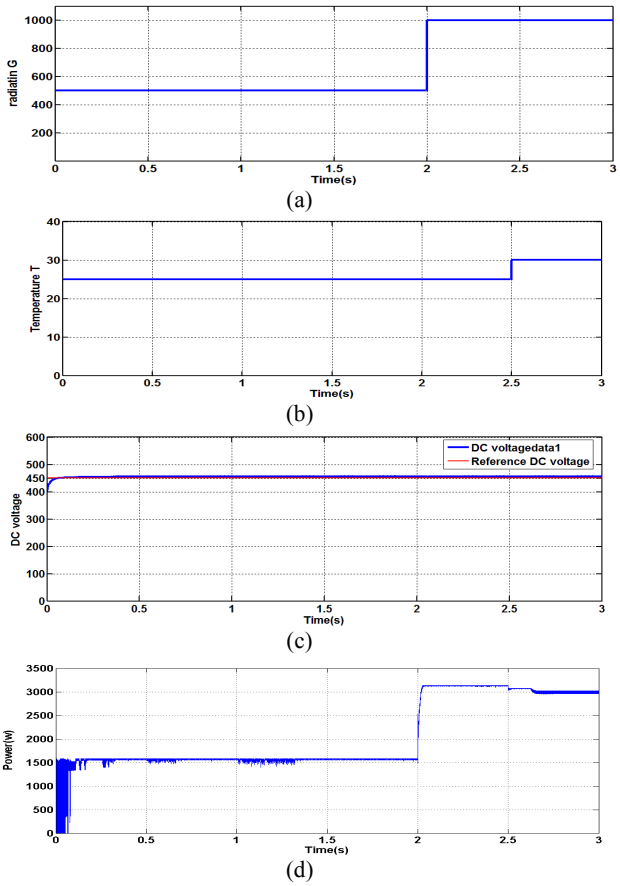

Fig.7. Simulation results of the designed interleaved boost converter and buck inverter. (a) Radiation, (b) Temperature, (c) DC voltage, (d) PV power

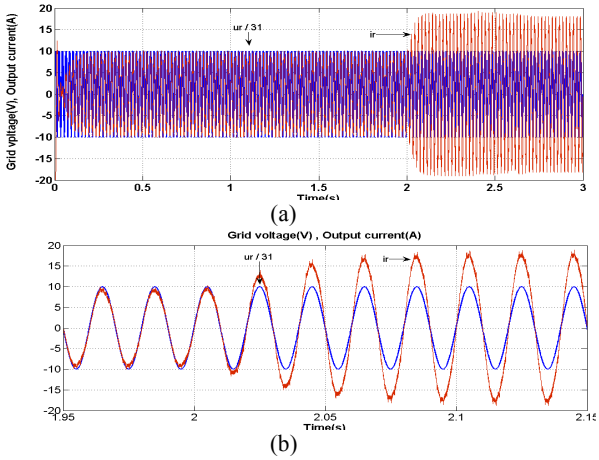

Fig.8. Simulation results of the designed interleaved boost converter and buck inverter.(a) Grid voltage and current, (b) Grid voltage and current [1.95 to 2.15s]

References

[1] Xiuhong Guo, Quanyuan Feng , "Passivity-based Controller Design for PWM DC/DC Buck Current Regulator", Proceedings of the World Congress on Engineering and Computer Science WCECS, San Francisco, USA, October 2008, pp. 875-878

[2] T. Ostrem, W. Sulkowski, L. E. Norum, and C. Wang, "Grid Connected Photovoltaic (PV) Inverter with Robust Phase-Locked Loop (PLL)", IEEE PES Transmission and Distribution Conference and Exposition Latin America, Caracas ,Venezuela, Aug. 2006, pp. 1-7

[3] Chen-Chi Chu, Chieh-Li Chen, "Robust maximum power point tracking method for photovoltaic cells: A sliding mode control approach", Solar Energy,Vol. 83 n.8, August 2009, pp. 1370-1378

[4] Guohui Zeng, Xiubin Zhang, Junhao Ying,Changan Ji ,"A Novel Intelligent Fuzzy Controller for MPPT in Grid-connected Photovoltaic Systems", Proc. of the 5th WSEAS/IASME Int. Conf. on Electric Power Systems, High Voltages, Electric Machines, Tenerife, Spain, December , 2005, pp. 515-519

[5] Trishan Esram,, Patrick L. Chapman, Comparison of Photovoltaic Array Maximum Power Point Tracking Techniques , IEEE Transaction on Energy Conversion, VOL. 22 n. 2, JUNE 2007, pp 439 – 449

[6] Peftitsis, D. Adamidis, G. Balouktsis, A. "A new MPPT method for Photovoltaic generation systems based on Hill Climbing algorithm," Electrical Machines, ICEM 2008. 18th International Conference , Sept. 2008, pp. 1-5

[7] N. Femia, G. Petrone, G. Spagnuolo, and M. Vitelli, "Optimization of Perturb and Observe maximum power point tracking method", Power Electronics, IEEE Transactions, Vol. 20, n.4, July 2005, pp. 963–973

[8] Jae Ho Lee; HyunSu Bae; Bo Hyung Cho, "Advanced Incremental Conductance MPPT Algorithm with a Variable Step Size", Power Electronics and Motion Control Conference EPE-PEMC 12th International, Sept 2006, pp. 603 - 607

[9] Nopporn Patcharaprakiti, Suttichai Premrudeepreechacharn, Yosanai Sriuthaisiriwong ,Maximum power point tracking using adaptive fuzzy logic control for grid-connected photovoltaic system, Renewable Energy, Vol 30 n.11, Sept 2005, pp. 1771-1788

[10] Jonathan W. Kimball, Philip T. Krein, "Digital Ripple Correlation Control for Photovoltaic Applications", Power Electronics Specialists Conference IEEE, Orlando, FL, June 2007, pp 1690 – 1694

[11] Trishan Esram, Jonathan W. Kimball, Philip T. Krein, Patrick L.Chapman and Pallab Midya, Dynamic Maximum Power Point Tracking of Photovoltaic Arrays Using Ripple Correlation Control, IEEE Transactions on power electronics, SEPT 2006, pp.1282 – 1291

[12] Liccardo, F.Marino, P.Torre, G.Triggianese, " Interleaved DC-DC converters for photovoltaics modules", Clean Electrical Power, ICCEP '07. International Conference, May 2007, pp. 201 – 207

[13] Khalil, H. K., 1996, Nonlinear Systems, 2nd ed.,Prentice Hall, New York, USA.

[14] Marcelo Gradella Villalva, Jonas Rafael Gazoli, and Ernesto Ruppert Filho, Comprehensive Approach to Modeling and Simulation of Photovoltaic Arrays, IEEE Transaction On Power Electronics, vol. 24 n. 5, May 2009, pp. 1198 –1208

[15] Campbell, R.C, " A Circuit-based Photovoltaic Array Model for Power System Studies", Power Symposium, NAPS '07. 39th North American, December 2007, pp. 97 – 101

[16] Carlos Meza, Domingo Biel, Juan Negroni, Francesc Guinjoan, "Boost-Buck Inverter Variable Structure Control for Grid-Connected Photovoltaic Systems with Sensorless MPPT", IEEE on Industrial Electronic ISIE, June 2005, Croatia, vol. 2, pp. 657 - 662

Hassan Abouobaida was born in Rabat, Morocco, in 1974. He received the « Diplôme d'ENSET » in Electrical Engineering from Ecole Normal Supérieur de l'Enseignement Technique Mohamedia in 1998, and the « Diplôme DESA », in Electrical Engineering from Ecole Mohammadia d'Ingénieur, Université Mohamed V , Rabat, Morocco, in 2007. He is currently teacher in IBN SINA Technical School, Kenitra , Morocco. His research interests power electronics, control systems and renewable energy.

Mohamed Cherkaoui was born in Marrakech, Morocco, in 1954. He received the diplôme d'ingénieur d'état degree from the Ecole Mohammadia, Rabat, Morocco, in 1979 and the M.Sc.A. and Ph.D. degrees from the Institut National Polytechnique de la Loraine, Nancy, France, in 1983 and 1990, respectively, all in Electrical Engineering. During 1990-1994, he was a Professor in Physical department, cadi Ayyad university, Marrakech, Morocco. In 1995, he joined the Department of Electrical Engineering, Ecole Mohammadia, Rabat, Morocco, where is currently a Professor and University Research Professor. His current research interests include renewable energy, motor drives and power system. Dr. Cherkaoui is a member of the IEEE.